Improvement of mechanical properties of parts produced from AlSi10Mg powder with use of SLS/SLM technology by densification of the product surface layer

Poprawa właściwości mechanicznych elementów wykonanych z proszku AlSi10Mg metodami SLS/SLM przez zagęszczenie warstwy wierzchniej spieków

ANDRZEJ STWORA
GRZEGORZ SKRABALAK
JOANNA MASZYBROCKA *

DOI: https://doi.org/10.17814/mechanik.2017.5-6.58

The paper presents results of experiments including application of finishing machining (turning and burnishing) of samples produced with SLS/SLM, as well as influence of the sample orientation against the surface of base plate during building process (0°, 45°, 90°) on tensile strength of the produced samples. There are also presented results of microstructure examination and results of density measurements. The paper also discusses the state of samples surface layer depending on the applied finishing method.
KEYWORDS: selective laser sintering/melting, SLS/SLM, additive manufacturing, surface layer, AlSi10Mg, burnishing, turning

Aluminum and silicon alloys (Al-Si) are widely used in the manufacturing industry. The components of Al-Si alloys are often produced in die casting and metal forming methods. Due to the low density (about 2.7 g/cm^3), good thermal conductivity and relatively good machinability (especially weldability), Al-Si alloys are commonly used in the industry: tooling (mold inserts with conformal cooling channels) [1, 2], electronic and machine (radiators and heat exchangers), aircraft (lightweight and durable openwork constructions) [3, 4]. Due to the increasing application field of Al-Si based materials, these alloys are also more often used in additive manufacturing (such as Selective Laser Sintering/Melting - SLS/SLM). Among others, AlSi10Mg and AlSi12Mg powders are usually used for this purpose.

Together with the growing possible application of additively manufactured components, there are observed increasing requirements concerning their properties in particular: improvement of accuracy, quality of surface topography and increasing mechanical strength. Applied technology of layer machining with usage of laser beam l implies problems of obtaining high mechanical strength [5-8] and good surface quality (at present *Ra* is 20÷50 µm). Results of the worldwide researches in the area of SLS/SLM [9-13] show that by compacting the samples and by modifying the sintering/melting process parameters, the strength of the components can be significantly improved. Unfortunately the surface quality can not be improved, what implies more demands for finishing machining. Since surfaces obtained by laser sintering are characterized by high roughness, cutting processes are used as the first phase for finishing. In order to improve the surface quality and mechanical properties, among others burnishing might be applied.

* mgr inż. Andrzej Stwora (andrzej.stwora@ios.krakow.pl), dr inż. Grzegorz Skrabalak (grzegorz.skrabalak@ios.krakow.pl), – Instytut Zaawansowanych Technologii Wytwarzania; dr Joanna Maszybrocka (joanna.maszybrocka@us.edu.pl – Instytut Nauki o Materiałach, Uniwersytet Śląski

Description of the research

Incremental manufacturing methods are commonly used for production of lightweight, openwork constructions. For this reason, during performed experiments, samples prepared with SLS/SLM were positioned at different angles (0÷90°) with respect to the surface of the base plate of the device.Test samples were prepared applying the SLS/SLM technique, taking into account their orientation in relation to the base plate: parallel to the base plate (0°), perpendicular to the base plate (90°) and 45° to the base plate [7, 8]. In addition, some of the samples were subjected to turning and burnishing to improve the quality of the outer surface and eliminate the pores therein. Prepared samples were tested for strength. For more complete analysis and full characterization of the material, the microstructure, density and surface topography (*Ra*, *Rz*) were examined.

The results will be the basis for the optimization of the SLS/SLM process parameters so that in the future, the lightweight components produced by this method are robust and of good quality.

AlSi10Mg powder with a mean grain size of 50 µm was used. This material is characterized by high thermal conductivity (about 200 W/m•K) and low specific weight (2.67 g/cm^3). This is a typical casting alloy with good strength and hardness, so it can be used to produce even heavy duty mechanical components. Since the elements made of this alloy are relatively light weight, it might be effectively used for production of to make elements of large dimensions, complex geometry and thin walls - for example, aerial parts, radiators. The chemical composition of the powder used is presented in Table I. Microphotographs of the AlSi10Mg powder are presented in Fig. 1. It can be seen that the powder is characterized by a large number of particles with a diameter of 30÷50 µm and irregular shape (although the powder is intended for the SLS/SLM process), which may adversely affect the structure of the samples,

including contributing to the formation of an increased number of pores (compared to samples made from spherical powders).

Test samples were prepared with the SLS/SLM technique using Renishaw AM250 equipped with a 400 watt fiber laser with a wavelength of 1060÷1070 nm. Technological parameters, presented in Table II, for preparing samples were developed basing on previous experiments [2, 11].

Test samples were prepared with different sintering orientation (0°, 45°, 90°) relative to the working plate (fig. 2) to determine the tensile strength of the specimens.

TABLE I. Chemical composition of AlSi10Mg powder

Al	Si	Fe	Cu	Mn	Mg	Ni	Zn	Pb	Sn	Ti
87,1÷89,35	9÷11	0,55	0,05	0,45	0,2÷0,45	0,05	0,10	0,05	0,05	0,15

TABLE II. Sintering parameters of test samples made using SLS/SLM technology

Laser power, W	400
Point distance, μm	75
Exposure time, μs	75
Hatch space, μm	165
Layer thickness, μm	50
Sintering strategy,	meander

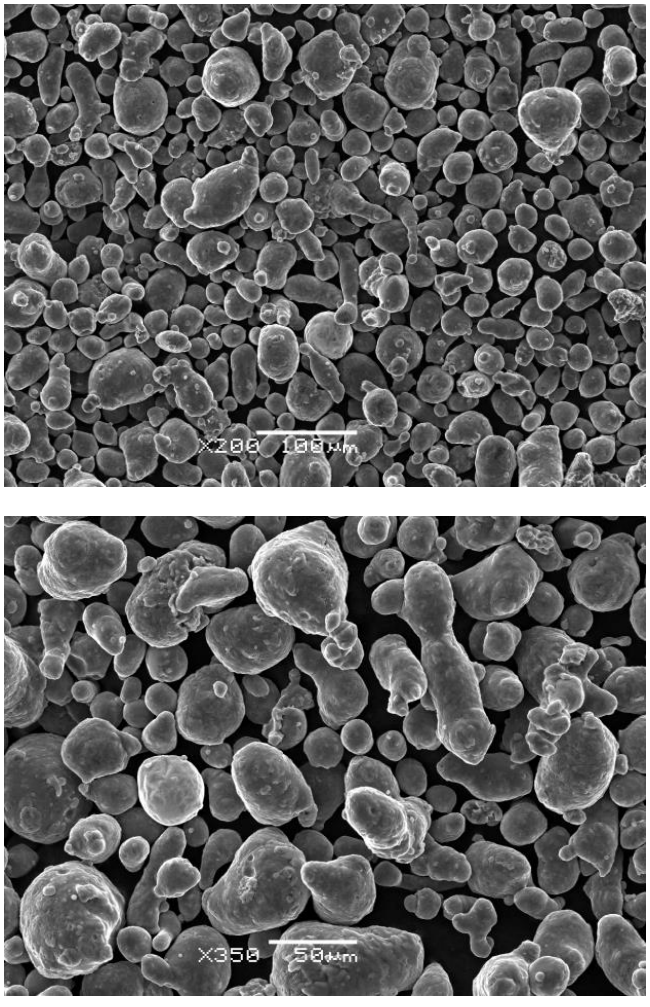

Fig. 1. SEM microphotography of AlSi10Mg powder in different magnifications

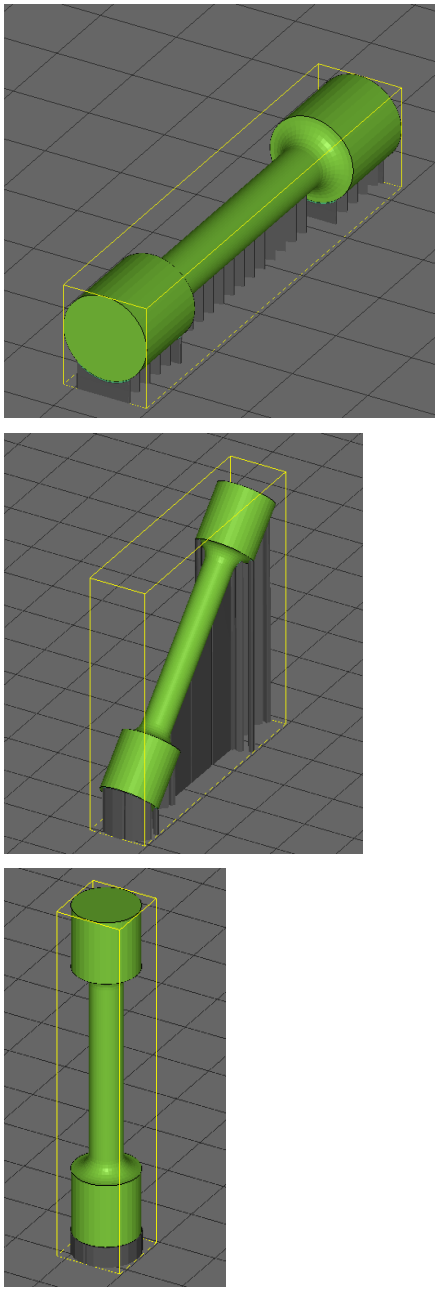

Fig. 2. Sample positioning at an angle 0°, 45° and 90° to the base plate

In order to check the density of the sinter and to examine their microstructure, 10 mm × 10 mm × 10 mm cubic samples were prepared (fig. 3). Wrecks were prepared using Keller's reagent. Prior to insertion into the microscope, the samples were purified in an ultrasonic cleaner.

The apparent density was measured by saturation in vacuum, according to PN-EN 632-2.

Scanning electron microscopy (SEM) analysis was performed using a JEOL JSM 6460LV microscope equipped with an Oxford Instruments EDS XDS spectrometer.

For the static tensile test, samples were prepared with the dimensions presented in fig. 4. Samples were tested according to PN-EN ISO 6892-1 on the Instron 5982 universal testing machine (fig. 5) [14], whose traverse speed was 1 mm/min.

The mechanical properties and microstructure of both raw samples (removed from the SLM machine) and samples after additional finishing machining were investigated.

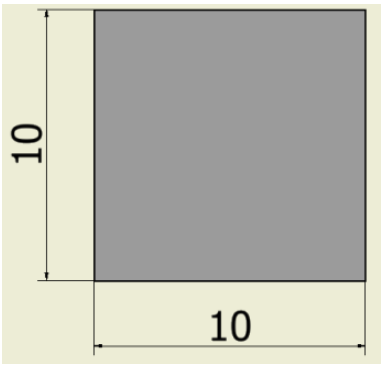

Fig. 3. Cross section of the sample for density measurements and microstructure investigations of sinter

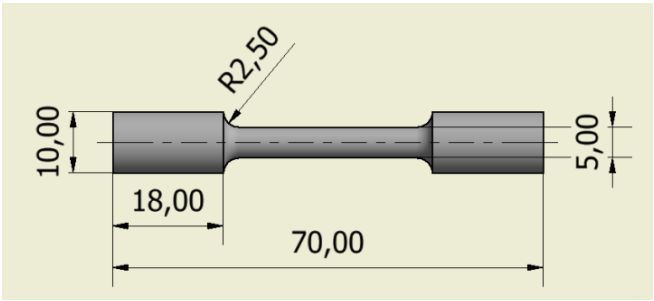

Fig. 4. Samples to perform a static tensile strength test

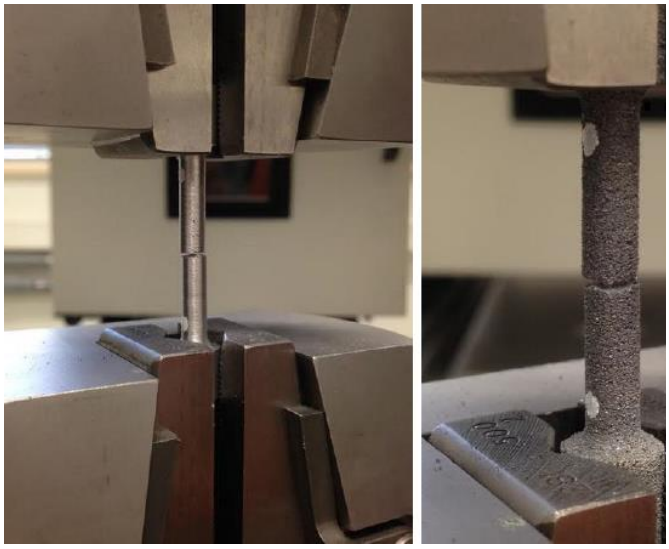

Fig. 5. Samples during tensile strength tests on the Instron 5982

Part of the samples were subjected to turning machining (fig. 6) - with a cutting speed p = 70 m/min, tool feedrate F = 0.14 mm/rev and cutting depth a_p = 0.2 mm - and burnishing (fig. 7). These operations aimed at both: reducing the surface roughness of the samples and eliminating the pores in the surface layer structure. As a pre-burnishing treatment, a hard turning method was used. Small feed rates and small cutting depths resulted in the removal of material and simultaneously pitting the pores, which resulted in increased strength of the sintered samples [15]. This phenomena results from the fact that both, burnishing tool and cutting tool, in contact with the workpiece, induces local elastic and plastic deformations under the influence of the pressure. Of course, in case of a turning lathe, where there is no tool rotation, unlike in case of roller-burnishing tool, changes in the top layer will be smaller (fig. 7). As a result of deformation there is a change in the crystallographic orientation of the grains and their original shape, leading to a decrease in roughness and material density in the surface layer. In addition, the grains are crushed, folded and elongated towards the largest deformations, forming crumb texture with anisotropy of mechanical properties. The plastic deformation occurs to a certain depth from the surface, which depends on the properties of the material and the technological parameters of the burnishing process (burn speed p = 40 m/min, feedrate F = 0.3 mm, tool penetration to the burnishing surface a_p = 0.3 mm).

Fig. 8 compares raw and finished samples.

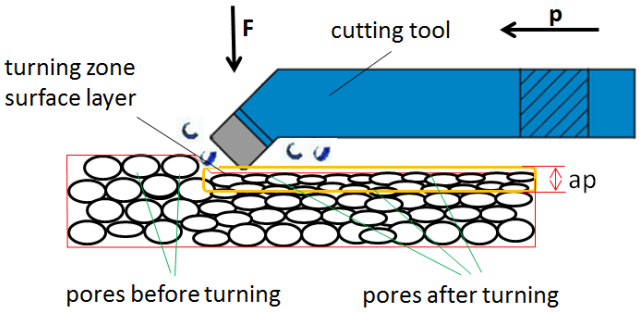

Fig. 6. Scheme of the plastic deformation (reduction of roughness, elimination of pores) in the surface of the sample during turning machining

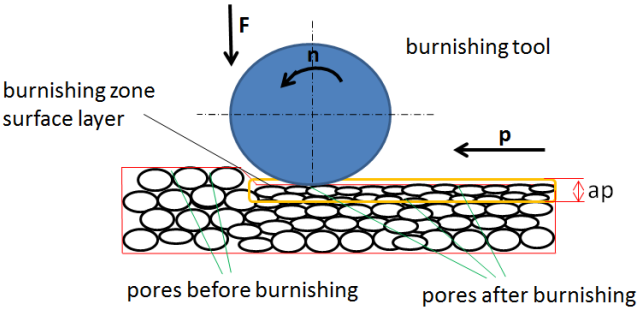

Fig. 7. Scheme of the plastic deformation (reduction of roughness, elimination of pores) in the surface of the sample during burnishing

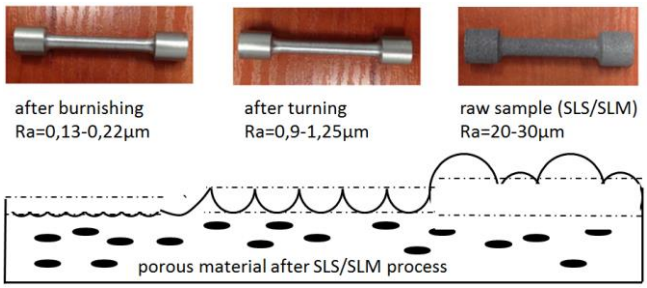

Fig. 8. Samples after burnishing, turning and sintering (raw)

Analysis of the results of microstructure studies

Qualitative studies of selected samples revealed internal defects/pores generated during SLS/SLM production. Although AlSi10Mg sintering experiments are conducted in argon atmosphere with an oxygen content of no more than 0.1%, the process of filling the chamber with powdered material can lead to the formation of oxides by contact of powder with atmospheric air. This fact might lead to existence of unprocessed oxides in the

sintered material, although high energy (400W) laser is used for SLS process. This problem was also mentioned, among others, by L. Thijs et al. [16] and E. Louvis et al. [17]. It is worth to emphasize that the pores are stochastic, and that the bond between the layers is unnoticeable, which proofs the good melting of the powder grains [2] and confirms the presence of oxides (fig. 9).

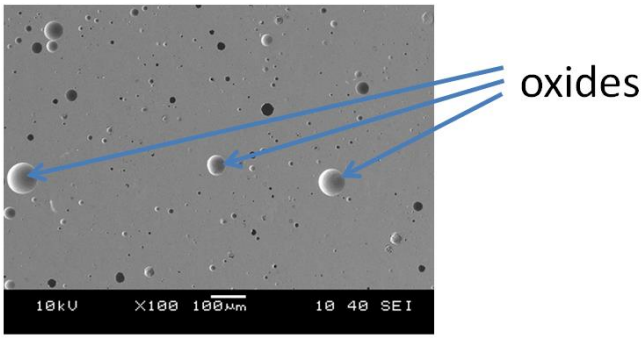

Fig. 9. Photo of a sectional microstructure of a sample made of AlSi10Mg material

Analysis of the microstructure of the samples confirms that hard turning causes reduction of the surface roughness and the number of pores in the surface layer (fig. 10), including closure of open pores. Even less porosity is observed in the surface layer finished with rolling burnishing.

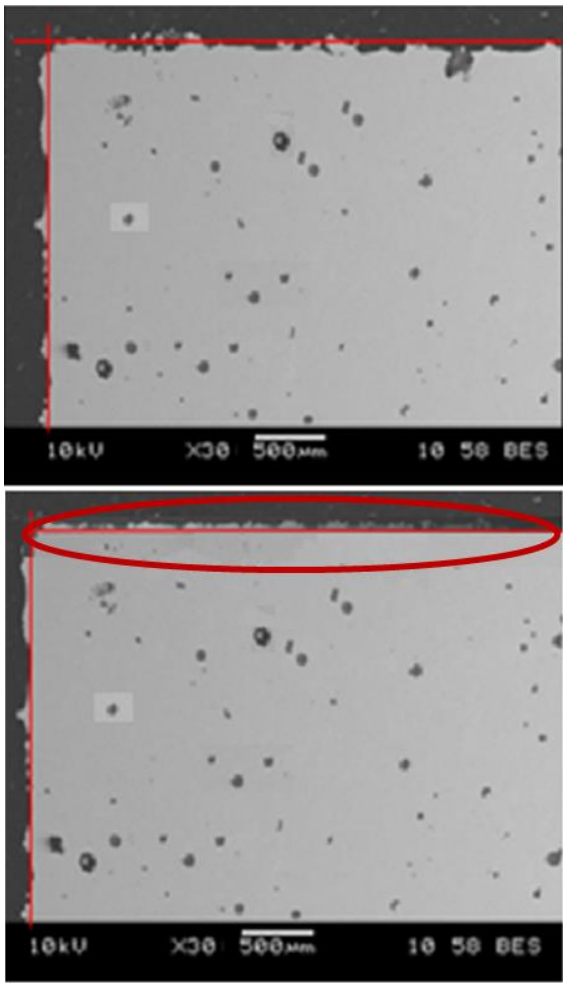

a)

b)

Fig. 10. Photo of the microstructure of the sample cross section: a) before turning, b) after turning

Fig. 11 shows the microstructure of the sample surface after finishing (after turning - fig. 11a) and raw samples (fig. 11c). Significant differences in the edges of the sample after turning (fig. 11b) and the unprocessed sample (fig. 11d) are noted in the pictures. It might be observed that finishing machining not only removes the outer layer of the not fully melted powder, but also causes crushing of grains in the newly created surface layer (especially visible as the regular edge on the samples fractures For unprocessed samples, there are large irregularities/bruises in the outer layer of the tested piece.

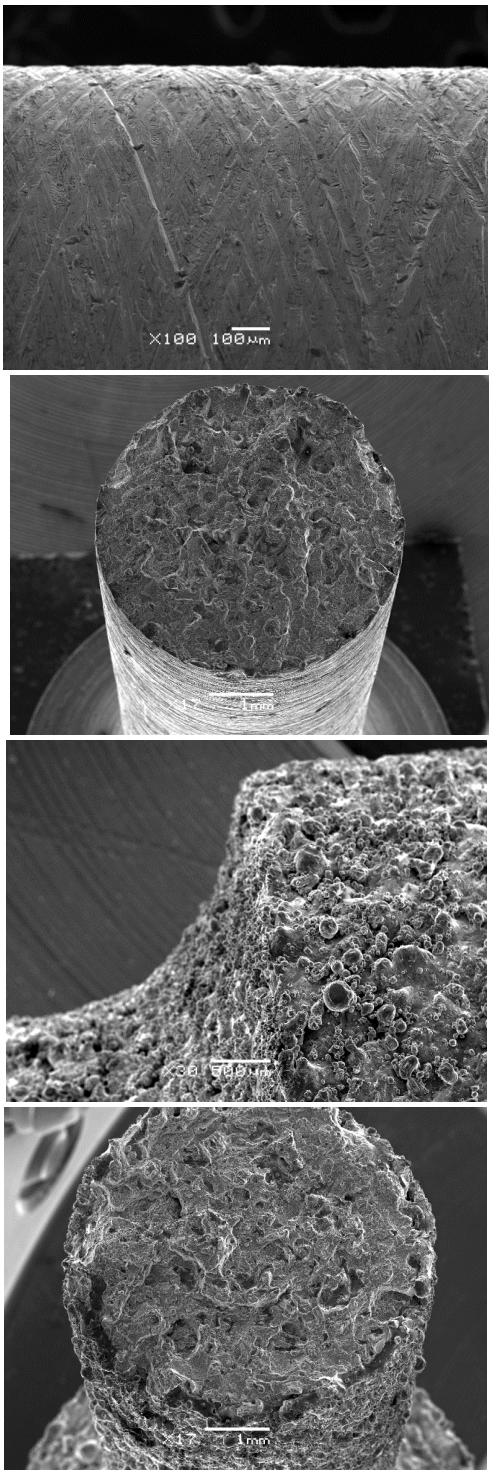

a)

b

c)

d)

Fig. 11. Side surface and morphology of the *XY* breakthrough (90° sample): sample after turning (a, b) and raw sample (c, d)

On the basis of the results of the density studies it was found that the samples made according to the selected parameters are characterized by a density of 2.47 g/cm^3, which is 92.5% of the density of cast materials (2.67 g/cm^3).

Surface microstructure analysis showed a significant reduction in the surface roughness of the sintered sample. Immediately after sintering, the *Ra* value was 20÷30 μm (fig. 12), after the turning process - 0.9÷1.25 μm, and after the burnishing process - 0.13÷0.22 μm (fig. 13).

It can be clearly stated that hard turning processes and rolling burnishing can significantly reduce the surface roughness of AlSi10Mg material. The use of additional machining is only possible with cylindrical components (fig. 14), which seems to be a major limitation.

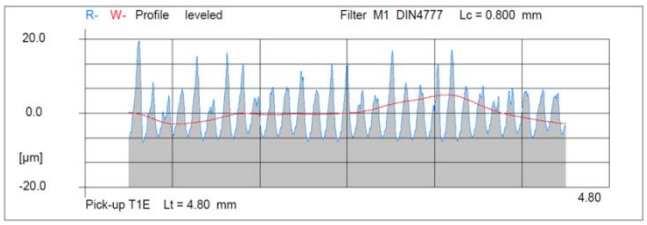

Fig. 12. Surface topography analysis of raw sample (after sintering)

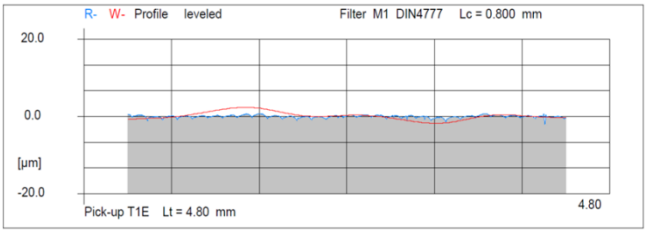

Fig. 13. Analysis of surface topography after burnishing

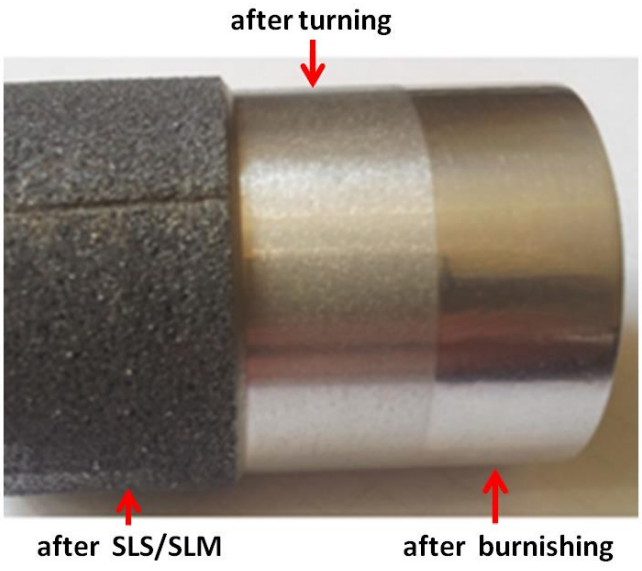

Fig. 14. Sample of AlSi10Mg material with specified areas after sintering, turning and burnishing

Analysis of tensile strength test results

The SLS/SLM samples were cut off from the base plate after the sintering process.

The first sample series (nine samples - three of each type: XY-R, 45-R, 90-R) was subjected to a static tensile strength test without any additional treatment.

The second set of samples (nine samples - three of each type: XY, 45, 90) was made with a 0.2 mm oversize and then machined (turning) to the nominal dimensions according to the dimensions necessary for standard tensile strength test..

In addition, there were three samples designated XY-N (oriented parallel to the plane of the base plate) and made with a 0.3 mm oversized finish which was subjected to a finishing machining- hard turning and burnishing.

The results obtained for samples from the first and second series (taking into account the sintering direction with respect to the working plate) are presented in Table III.

TABLE III. Tensile strength and deformation of SLS/SLM samples, prior to turning and after turning, depending on the direction of sintering

Direction of processing	Tensile strength, R_m, MPa	Average absolute deviation, MPa	Tensile strain, ε, %	Average absolute deviation, %
XY	260,25	1,16	3,38	0,46
45	271,47	1,27	2,37	0,27
90	292,12	0,58	1,50	0,03
XY-R	227,61	14,46	3,04	0,16
45-R	253,02	15,27	2,20	0,10
90-R	264,36	6,51	1,43	0,02

When analyzing the results (fig. 15 and fig. 16), it was noted that the turning samples exhibited better tensile strength than raw samples. Furthermore, they are subjected to higher deformation (elongation) prior to being torn apart.. It is worth to notice that also additional finishing machining – burnishing after turning significantly improves the samples tensile strength (fig. 16) by approximately 40% compared to the sample after hard turning.

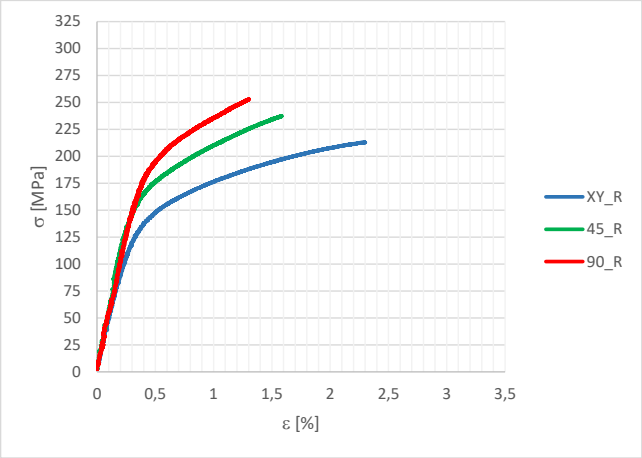

Fig. 15. Tensile strength and deformation of unfinished SLS/SLM samples, depending on the sintering direction relative to the working plate (0°, 45°, 90°)

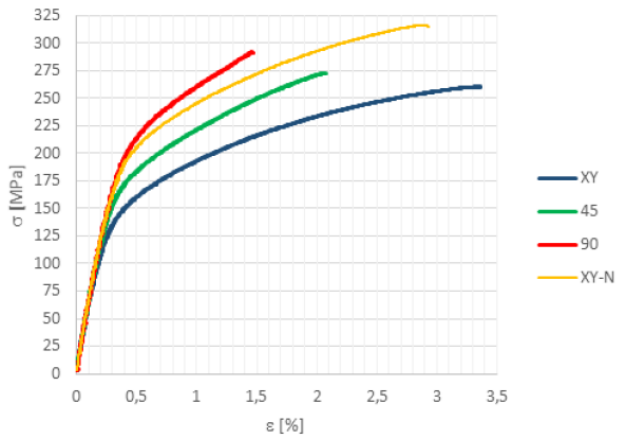

Fig. 16. Tensile strength and deformation of SLS/SLM slabs subjected to turning, depending on the sintering direction relative to the working plate (0°, 45°, 90°). The yellow curve represents the samples after burnishing

Conclusions

The presented microstructure and density studies of AlSi10Mg alloys have confirmed that the increase in density and the reduction of porosity in the surface layer of SLS/SLM produced samples have significant effect on their strength.

Application of hard turning and burnishing machining allows to significantly reduce the porosity and kneading of the pores, which directly affects ed the increase of the mechanical strength of the samples tested.

Oxides produced as a results of contact of reactive powders, i.e. AlSi10Mg and Ti6Al4V, with oxygen require a higher melting temperature than non-oxidized material.

The high content of oxides in Al-Si material results in not fully melted areas with high porosity, which is reflects in the lower tensile strength and worse quality of the components produced. The high concentration of pores in the small sinter area causes deterioration of the mechanical strength of the element. Relatively high concentration of pores associated with the presence of unprocessed, oxidized powdered grains causes also weakening of the surface layer. It might be especially observed during finishing machining of the samples – sand blasting, when in high porous surface layer areas large cracks are created as a result of contact of material with abrasive grains.

REFERENCES

1. Bremen S., Meiners W., Diatlov A. “Selective laser melting – additive manufacturing for series production on the future”.
2. Stwora A., Skrabalak G. „Wpływ parametrów technologicznych procesu selektywnego topienia laserowego na wybrane właściwości elementów wykonanych z proszków stopu AlSi10Mg”. *Mechanik.* 3 (2016): pages 206–209.
3. Qiu C., Yue S., Adkins N.J.E., Ward M., Hassanin H., Lee P.D., Withers P.J., Attallah M.M. “Influence of processing conditions on strut structure and compressive properties of cellular lattice structures fabricated by selective laser melting”. *Materials Science and Engineering: A.* 628 (2015): pages 188–197.
4. Leary M., Mazur M., Elambasseril J., McMillan M., Chirent T., Sun Y., Qian M., Easton M., Brandt M. “Selective laser melting (SLM) of AlSi12Mg lattice structures”. *Materials and Design*. 98 (2016): pages 344–357.
5. Maskery I., Aremu A.O., Simonelli M., Tuck C., Wildman R.D., Ashcroft I.A., Hague R. “Mechanical properties of Ti-6Al-4V selectively laser melted parts with body-centred-cubic lattices of varying cell size”. *Experimental Mechanics*. 55, 7 (2015): pages 1261–1272.
6. Aboulkhair N.T., Everitt N.M., Ashcroft I., Tuck C. “Reducing porosity in AlSi10Mg parts processed by selective laser melting”. *Additive Manufacturing*. 1–4 (2014): pages 77–86.
7. Kempena K., Thijsb L., Van Humbeeckb J., Kruth J.-P. “Mechanical properties of AlSi10Mg produced by selective laser melting”. *Physics Procedia*. 39 (2012): pages 439–446.
8. Brandl E., Heckenberger U., Holzinger V., Buchbinder D. “Additive manufactured AlSi10Mg samples using selective laser melting (SLM): microstructure, high cycle fatigue and fracture behavior”. *Materials and Design*. 34 (2012): pages 159–169.
9. Buchbinder D., Schleifenbaum H., Heidrich S., Meiners W., Bültmann J. “High power selective laser melting (HP SLM) of aluminum parts”. *Physics Procedia*. *Part A*. 12 (2011): pages 271–278.
10. Olakanmi E.O., Cochrane R.F., Dalgarno K.W. “Densification mechanism and microstructural evolution in selective laser sintering of Al-12Si powders”. *Journal of Materials Processing Technology*. 211 (2011): pages 113–121.
11. Stwora A., Skrabalak G. “Influence of selected parameters of selective laser sintering process on properties of sintered materials”. *Journal of Achievements in Material Manufacturing Engineering*. 61, 2 (2013): pages 375–380.
12. Kempen K., Thijs L., Yasa E., Badrossamay M., Verheecke W., Kruth J. “Microstructural analysis and process optimization for selective laser melting of AlSi10Mg”. *Solid Freeform Fabrication Symposium Proceedings*. Austin, Texas, USA, 8–10 August 2011.
13. Aboulkhair N.T., Stephens A., Maskery I., Tuck C., Ashcroft I., Everitt N.M. “Mechanical properties of selective laser melted AlSi10Mg: nano, micro, and macro properties”. *Proc. of Solid Freeform Fabrication Symposium*. *Vol. 1. Intergovernmental Panel on Climate Change.* Cambridge: Cambridge University Press, 2015, s. 1–30.
14. PN-EN ISO 6892-1:2016:09 (wersja angielska). Metale – Próba rozciągania – Część 1: Metoda badania w temperaturze pokojowej.
15. Dobrzyński M., Przybylski W., Waszczur P. „Ocena parametrów chropowatości powierzchni toczonych otworów w kołach zębatych obrabianych nagniataniem”. *Tribologia.* 6 (2012): pages 61–68.
16. Thijs L., Kempen K., Kruth J.P., Humbeeck J.V. “Fine-structured aluminium products with controllable texture by selective laser melting of pre-alloyed AlSi10Mg powder”. *Acta Materialia*. 61, 5 (2013): pages 1809–1819.
17. Louvis E., Fox P., Sutcliffe C.J. “Selective laser melting of aluminium components”. *Journal of Materials Processing Technology*. 211 (2011): pages 275–284.